A Channel-Estimation and Data-Detection Scheme for Multiuser MIMO-CDMA Systems in Fading Channels

Ayman Assra, Walaa Hamouda, *Senior Member, IEEE*, and
Amr Youssef, *Senior Member, IEEE*

***Abstract*—In this paper, we examine the effect of channel estimation errors on the performance of multiple-input–multiple-output (MIMO) systems that employ code-division multiple-access (CDMA) transmission. Channel estimation based on training techniques has widely been considered throughout the literature. However, employing these training techniques in MIMO-CDMA systems degrades system performance due to multiuser interference. This degradation is clear as the diversity advantage of the MIMO system diminishes with the increased level of interference. As a remedy to this problem, we propose a channel-estimation and data-detection scheme based on the superimposed training technique for space-time spreading systems. The proposed scheme enhances the performance of the space-time system by eliminating the interference effect from both the channel and data estimates using two decorrelators: channel and data decorrelators. We investigate the performance of the proposed estimation technique considering an asynchronous CDMA uplink transmission over frequency-selective slow-fading channels. In particular, we analyze the bit-error-rate (BER) performance of the multiuser system with two-transmit-antenna and V-receive-antenna configuration over Rayleigh fading channels. Compared with other conventional estimation techniques, our results show that the proposed estimation technique is more robust to channel-estimation errors. Furthermore, both simulations and analytical results indicate that full system diversity is achieved.**

***Index Terms*—Channel estimation, code-division multiple-access (CDMA), multiple-input–multiple-output (MIMO), superimposed training.**

I. Introduction

SUPPORTING the expected high data rates required by wireless Internet and high-speed multimedia services is one of the basic requirements in broadband mobile wireless systems. In the design of such systems, two critical performance- and capacity-limiting factors are multipath fading and multiaccess interference [1]. Recently, space-time coding (STC) techniques have extensively been studied to combat fading effects and improve system capacity [2], [3]. In these STC techniques, multiple signal transmissions are combined with the appropriate signal processing at the receiver side to provide diversity and/or coding gains. Examples of these STC techniques are space-time trellis coding [4] and space-time block coding [5], [6]. The former is a generalization of trellis coding to multiple transmit and receive antennas, while the latter is a generalization of Alamouti's dual-transmit diversity scheme [5] to multiple transmit antennas.

Code-division multiple access (CDMA) is seen as one of the generic multiple-access schemes in the second and third generations of wireless communication systems [7]. Despite its promises, CDMA systems have fundamental difficulties when utilized in wideband wireless communications. As the system bandwidth increases, there are more resolvable paths with different delays. Hence, the received CDMA signals suffer from interchip interference, causing significant cross correlation among users' signature waveforms. The application of STC to CDMA systems has previously been investigated in [8], where a space-time spreading (STS) scheme was proposed for both the uplinks and downlinks of a direct-sequence (DS) CDMA system. This scheme has the advantage of maintaining the full system diversity with no waste of system resources [9].

In multiple-input–multiple-output (MIMO) systems, channel estimation plays a crucial role in determining the system performance (e.g., [10]–[14] and the references therein). While the majority of the works in MIMO assume perfect channel estimation, relatively few researchers have investigated the effect of channel-estimation errors and possible estimation techniques. For instance, Sharma and Chockalingam [10] have investigated the performance of space-time coded systems in CDMA considering channel estimation errors. In that, the authors considered the performance of the maximum-likelihood receiver in synchronous CDMA systems over flat-fading channels. Furthermore, Gao *et al.* [14] have considered the problem of channel estimation in MIMO single-carrier single-user systems. They proposed an optimal minimum-mean-square error (MMSE) channel-estimation technique for frequency-selective fading channels.

In conventional training-based approaches, a distinct training sequence, which is known to the receiver, is time multiplexed with the data sequence and transmitted from the corresponding antenna, which limits the spectral efficiency of the system [7]. Additionally, if the time variations of the channel are fast,

Manuscript received March 31, 2009; revised January 19, 2010 and March 1, 2010; accepted March 8, 2010. Date of publication April 5, 2010; date of current version July 16, 2010. The review of this paper was coordinated by Prof. C. P. Oestges.

A. Assra and W. Hamouda are with the Department of Electrical and Computer Engineering, Concordia University, Montreal, QC H3G 1M8, Canada (e-mail: a_assra@ece.concordia.ca; hamouda@ece.concordia.ca).

A. Youssef is with the Concordia Institute for Information Systems Engineering, Concordia University, Montreal, QC H3G 1M8, Canada (e-mail: youssef@ece.concordia.ca).

Color versions of one or more of the figures in this paper are available online at http://ieeexplore.ieee.org.

Digital Object Identifier 10.1109/TVT.2010.2047417

such an approach is inefficient as it requires training to be repeatedly performed, which limits the available time for data transmission. An alternative technique, which is referred to as blind channel estimation, can estimate the channel while the information signals are being transmitted [13]. These blind techniques have the advantage of improved bandwidth utilization at the expense of higher computational complexity. As a solution to the complexity problem, one can employ semiblind channel-estimation techniques. In this case, the channel is estimated not only by using known data but also through the observation corresponding to the unknown data [12]. More recently, a superimposed training-based approach has been explored where a distinct training sequence is added to the data sequence before modulation and transmission from the corresponding antenna. This estimation technique is known to offer relatively large bandwidth utilization [15]. For example, in [11], the authors examined the performance of superimposed training for MIMO channel estimation in single-user systems where a linear MMSE equalizer is introduced. Along the same lines, Meng *et al.* [15] have proposed an iterative channel-estimation and detection scheme based on the superimposed training technique for single-input–multiple-output systems.

In [16], Chong and Milstein employed the training-based technique on an STS system with dual-transmit and dual-receive diversity. In their work, the channel estimation was based on employing distinct pilot spreading codes on STS signals transmitted from different antennas. With the help of these pilot signals, the channel coefficients are estimated using a conventional rake receiver. These channel estimates are then used to combine the received signals in a rake-like space-time combiner for final data estimates. It is noted that both data and channel estimates suffer from intersymbol interference (ISI) and multiaccess interference (MAI). In light of this, we propose an enhanced channel-estimation and data-detection scheme based on the superimposed training-based approach. The proposed scheme is shown to enhance the performance by eliminating the MAI effect from both the channel and data estimates by employing channel and data decorrelators. Considering an uplink asynchronous CDMA system with K active users, we analyze the performance of the proposed estimation technique in frequency-selective slow-fading channels. We also consider an antenna configuration of two transmit antennas at the mobile and V receive antennas at the receiver base station. In our analysis, we obtain a closed-form expression for the probability of bit error as a function of the system parameters. Furthermore, we also provide a novel technique to calculate the bit error rate (BER), which is potentially of wider application. To evaluate the probability of error, we first obtain the probability density function (pdf) of the decision variable at the output of the space-time combiner. This pdf is then used to evaluate the average BER of the underlying space-time system. In our analysis, we consider the effect of correlation among different channel estimates at the multiuser detector output. The accuracy of the derived analytical results is verified by comparison with the simulated ones. From both simulations and analytical results, we show that the proposed estimation scheme achieves performance that is very close to the perfect-estimation case. More importantly, the results reveal that the full system diversity is achieved in the frequency-selective channel.

The remainder of this paper is organized as follows. The space-time system model used in our analysis is described in the following section. The channel-estimation and detection scheme is discussed in Sections III and IV. In Section V, the performance of the proposed estimation technique is analyzed in terms of the average BER. In Section VI, simulations and analytical results are presented. Finally, conclusions are drawn in Section VII.

II. System Model

The transmit-diversity scheme considered in our work consists of two transmit antennas at the mobile station and V receive antennas at the base station. The system block diagram for the kth transmitting user is shown in Fig. 1, where real-valued data symbols using binary phase-shift keying baseband modulation and real-valued spreading are assumed [9]. We consider the original STS scheme proposed in [8] with two spreading codes per user. As seen in Fig. 1, following the STS, two pilot spreading codes are assigned to each user for the purpose of channel estimation. Each pilot sequence is added (superimposed) on the STS signal before transmission from the corresponding antenna. We also consider an uplink asynchronous transmission from K users over a frequency-selective slow-fading channel (see Fig. 2), where the fading coefficients are fixed for the duration of an M-symbol data block but independently change from one block to another. Given the space-time scheme in [8], the duration of the space-time codeword is $T_s = 2T_b$, where T_b is the bit duration. The received complex low-pass equivalent signal at the vth receive antenna is given by

$$\begin{aligned} r^v(t) = \sum_{k=1}^{K}\sum_{l=1}^{L}\sum_{m=0}^{M-1} & h_{1l}^{k,v} \\ & \times \left[\sqrt{\frac{\rho_p}{2}}P_{k1}(t - mT_s - \tau_k - \tilde{\tau}_l)\right. \\ & \quad + \sqrt{\frac{\rho_d}{2}}\left(b_{k1}[m]c_{k1}(t - mT_s - \tau_k - \tilde{\tau}_l)\right. \\ & \quad \left.\left. + b_{k2}[m]c_{k2}\left(t - mT_s - \tau_k - \tilde{\tau}_l\right)\right)\right] \\ & + h_{2l}^{k,v}\left[\sqrt{\frac{\rho_p}{2}}P_{k2}(t - mT_s - \tau_k - \tilde{\tau}_l)\right. \\ & \quad + \sqrt{\frac{\rho_d}{2}}\left(b_{k2}[m]c_{k1}(t - mT_s - \tau_k - \tilde{\tau}_l)\right. \\ & \quad \left.\left. - b_{k1}[m]c_{k2}\left(t - mT_s - \tau_k - \tilde{\tau}_l\right)\right)\right] + n^v(t) \end{aligned} \tag{1}$$

where ρ_p and ρ_d represent the pilot and data SNRs, respectively. The data bits $b_{k1}[m]$ and $b_{k2}[m]$ represent the odd and even data streams of the kth user within the mth codeword interval. In (1), $c_{k1}(t)$ and $c_{k2}(t)$ are the kth user's data-spreading sequences

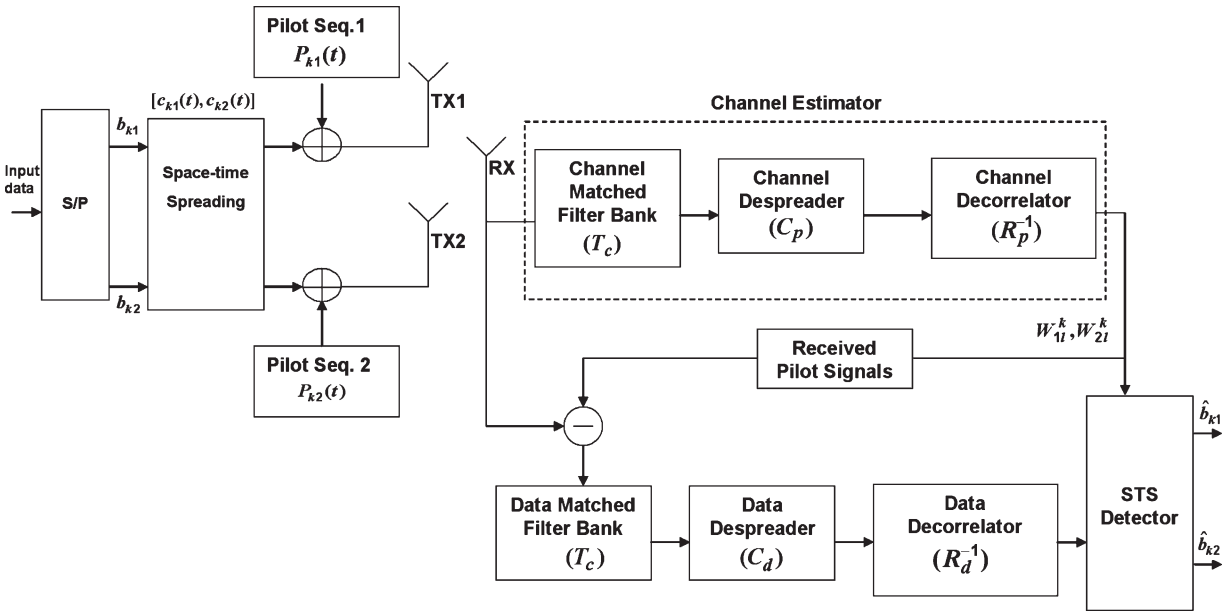

Fig. 1. Block diagram of the pilot-sequence-assisted STS transmission system corresponding to a single receive antenna.

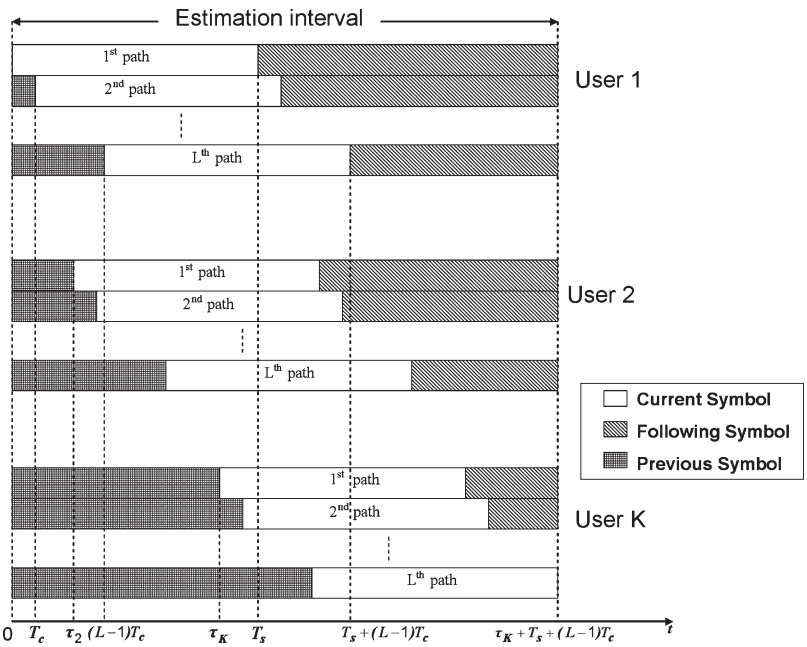

Fig. 2. Asynchronous transmission of K code sequences, each having a period $T_s = 2N$ chips, over a frequency-selective fading channel with L resolvable paths. The estimation interval is $T_s + \tau_K + (L-1)T_c$.

with processing gain $2N$, where $N = T_b/T_c$ represents the number of chips per bit, and T_c is the chip duration. The two pilot spreading sequences, i.e., $P_{k1}(t)$ and $P_{k2}(t)$, assigned to the kth user have a period of $2T_b$. In our analysis, we assume that the pilot and data spreading sequences assigned to the K users are mutually orthogonal at the transmitter side. However, due to asynchronous transmission, this orthogonality condition between codes is no longer valid at the receiver side. τ_k represents the transmit delay of the kth user's signal, which is assumed to be a multiple of chip periods within T_s. $\tilde{\tau}_l$ is the lth path delay ($\tilde{\tau}_l = lT_c$), $h_{il}^{k,v}$, $i = 1, 2$ is the channel coefficient corresponding to the kth user and lth path from the ith transmit antenna to vth receive antenna, and L is the total number of resolvable paths. These fading coefficients are modeled as independent complex Gaussian random variables with zero mean and variance $\sigma_h^2 = (1/L)$. We also consider a time-invariant channe l over the duration of an M-symbol data block. The noise $n^v(t)$ is Gaussian with zero mean and unit variance. At the receiver, the received signal is first sent to a channel estimator, where the path gain estimates $\{W_{il}^{k,v}, W_{il}^{k,v}\}$ of the lth path between transmit antenna $i = 1$ and 2 and receive antenna v are obtained. Then, the STS signals are detected using the estimated path gains. The receiver structure is further illustrated in the following sections.

III. Channel Estimation

At the receiver side, the received signal at each receive antenna is chip-matched filtered, sampled at a rate $1/T_c$, and accumulated over an observation interval of $(2N+\tau_{\max}+L-1)$ chips corresponding to the first symbol of the received data block for the K-user system. The $(\tau_{\max}+L-1)$ samples are due to the maximum multipath delay (i.e., delay of the Lth path) corresponding to the user with the maximum transmit delay $\tau_{\max}$. We consider a slow-fading channel where the channel is fixed for the frame duration but independently changes from one frame to another. To simplify the analysis, we neglect the interference effect from the previous and following data frames on the channel estimation process. Without loss of generality, we consider the first symbol observation interval of the transmitted data block in the channel-estimation process.

Fig. 2 shows a block diagram of the asynchronous transmission of K user code sequences, each with a period of $T_s=2N$ chips over a frequency-selective fading channel with L resolvable paths. Without loss of generality, we assume that the users' delays are arranged in ascending order, where $\tau_1=0\le\ldots\le\tau_k\le\ldots\le\tau_K\le T_s$ [17]. As shown, the estimation interval corresponding to the mth STS symbol interval $(m=0,1,\ldots,M-1)$ starts from the first path of the first user corresponding to the mth transmission period (i.e., τ_1 represents the minimum user delay $(\tau_1=0)$) to the end of the Lth path of the Kth user's mth symbol (τ_K is the maximum user delay $(\tau_K=\tau_{\max})$). Assuming perfect knowledge of the users' delays, one can construct the code matrices corresponding to the current, following, or previous symbol transmissions within the observation interval.

Let $\mathbf{y}^v[0]$ denote the observation vector at the vth receive antenna containing all samples related to the STS symbols transmitted by the K users within the observation interval. Then

$$\mathbf{y}^v[0]=\mathbf{C}[0]\mathbf{H}^v\mathbf{b}[0]+\mathbf{C}[1]\mathbf{H}^v\mathbf{b}[1]+\mathbf{n}^v[0] \tag{2}$$

where $\mathbf{C}[0]=[\mathbf{C}_1[0],\mathbf{C}_2[0],\ldots,\mathbf{C}_K[0]]$ represents the code matrix corresponding to the current received symbols $\mathbf{b}[0]$ within the observation interval. The submatrix $\mathbf{C}_k[0]$, $(k=1,2,\ldots,K)$ is a $[(2N+L-1+\tau_{\max})\times 4L]$ matrix containing the pilot and data sequences of user k associated with the L resolvable paths. In the same way, $\mathbf{C}[1]=[\mathbf{C}_1[1],\mathbf{C}_2[1],\ldots,\mathbf{C}_K[1]]$ represents the code matrix of the following received symbols $\mathbf{b}[1]$ within the observation interval. $\mathbf{C}_k[1]$ $(k=1,2,\ldots,K)$ is a $[(2N+L-1+\tau_{\max})\times 4L]$ matrix consisting of the pilot and data code sequences of user k associated with the following STS symbol within the current observation window. The definition of these matrices is given in Appendix A. The second term in the right-hand side of (2) represents the interference due to the following symbols $\mathbf{b}[1]$ of the K-user system. In (2), $\mathbf{H}^v$ is the channel-impulse response of the K-user system at the vth receive antenna and is defined by

$$\mathbf{H}^v=\operatorname{diag}\{\mathbf{H}_1^v,\mathbf{H}_2^v,\ldots,\mathbf{H}_K^v\}$$

where

$$\mathbf{H}_k^v=\left[\mathbf{H}_k^{vT}(1),\mathbf{H}_k^{vT}(2),\ldots,\mathbf{H}_k^{vT}(L)\right]^T,\qquad k=1,2,\ldots K$$

and the superscript T denotes transpose. $\mathbf{H}_k^v(l)$ $(l=1,2,\ldots,L)$ is determined according to the STS scheme in [8]. Here, $\mathbf{H}_k^v(l)$ is modified to include the effect of pilot transmission as follows:

$$\mathbf{H}_k^v(l)=\begin{bmatrix} h_{1l}^{k,v} & 0 & 0 & 0\\ 0 & h_{2l}^{k,v} & 0 & 0\\ 0 & 0 & h_{1l}^{k,v} & h_{2l}^{k,v}\\ 0 & 0 & -h_{2l}^{k,v} & h_{1l}^{k,v}\end{bmatrix}.$$

The transmitted data vector from the K users during the mth symbol duration $\mathbf{b}[m]$ is given by

$$\mathbf{b}[m]=\left[\mathbf{b}_1^T[m],\mathbf{b}_2^T[m],\ldots,\mathbf{b}_K^T[m]\right]^T \qquad m=0,1,\ldots,M-1$$

where

$$\mathbf{b}_k[m]=\left[\sqrt{\frac{\rho_p}{2}},\sqrt{\frac{\rho_p}{2}},\sqrt{\frac{\rho_d}{2}}b_{k1}[m],\sqrt{\frac{\rho_d}{2}}b_{k2}[m]\right]^T \qquad k=1,2,\ldots,K.$$

Finally, in (2), $\mathbf{n}^v[0]$ is a $[(2N+L-1+\tau_{\max})\times 1]$ vector representing the additive white Gaussian noise samples at the vth receive antenna, each with zero mean and unit variance. From (2), the received signal can be represented in a more compact form as

$$\mathbf{y}^v[0]=\mathbf{C}_p\mathbf{H}_p^v\mathbf{b}+\mathbf{n}^v[0] \tag{3}$$

where

$$\mathbf{C}_p=[\mathbf{C}[0],\mathbf{C}[1]],\mathbf{H}_p^v=\mathbf{I}_2\otimes\mathbf{H}^v,\mathbf{b}=\left[\mathbf{b}[0]^T,\mathbf{b}[1]^T\right]^T$$

and $\otimes$ denotes *Kronecker product* operation [18]. After the sampling and despreading of the received signal $\mathbf{y}^v[0]$ with the pilot and data code matrix $\mathbf{C}_p$, the output is given by

$$\mathbf{y}_c^v[0]=\mathbf{R}_p\mathbf{H}_p^v\mathbf{b}+\mathbf{N}_{cc}^v[0] \tag{4}$$

where $\mathbf{R}_p=\mathbf{C}_p^H\mathbf{C}_p$ is the pilot and data cross-correlation matrix, $\mathbf{N}_{cc}^v[0]$ is modeled as $N_c\,(\mathbf{0},\mathbf{R}_p)$ (zero-mean complex Gaussian vector with covariance $\mathbf{R}_p$), and H denotes Hermitian transpose. To estimate the covariance matrix $\mathbf{R}_p$, we assume that the users' delays are known at the receiver and the channel coefficients are constant within a data block of M symbols, i.e., quasi-static fading channel. Note that the authors in [16] have based their channel estimation on the channel despreader output $\mathbf{y}_c^v[0]$. That is, the channel estimation in [16] treats the multiuser interference and ISI as background noise. Hence, the error signal in the channel estimates is affected by the presence of ISI, MAI, and thermal noise. The self-interference between the two pilot signals of each user was also neglected in [16]. Here, we consider an asynchronous uplink channel where multiuser interference can limit the system performance. However, to overcome the effects of multiuser interference resulting from the asynchronous transmission, we employ, after the despreader, a decorrelator detector at each receive antenna for channel estimation. This will show to improve the

reliability of the estimation process. In this case, the output of the vth channel decorrelator is given by

$$\mathbf{y}_d^v[0] = \mathbf{H}_p^v \mathbf{b} + \mathbf{N}_{cd}^v[0] \tag{5}$$

where $\mathbf{N}_{cd}[0]$ is $N_c(\mathbf{0}, \mathbf{R}_p^{-H})$. Note that the cross-correlation matrix inversion is based on the pseudoinverse or the *Moore–Penrose* generalized inverse [19], which can be calculated using the singular value decomposition in $O(L^3K^3)$ operations [20]. Since this is implemented at each receive antenna, the total number of arithmetic operations needed by the overall removal operation is $O(VL^3K^3)$. For more details on the generalization of the decorrelator detector when $\mathbf{R}_p$ is rank deficient, see [21, p. 241–242]. From (5), the first $4LK$ elements are then chosen from the vth decorrelator output vector $\mathbf{y}_d^v[0]$ for estimating the channel coefficients at the vth receive antenna, yielding

$$\begin{aligned} W_{1l}^{k,v} &= Bh_{1l}^{k,v} + w_{1l}^{k,v}, \\ W_{2l}^{k,v} &= Bh_{2l}^{k,v} + w_{2l}^{k,v}, \qquad k = 1, 2, \ldots, K \quad l = 1, 2, \ldots, L \end{aligned} \tag{6}$$

where $B = \sqrt{(\rho_p/2)}$, $w_{1l}^{k,v}$ and $w_{2l}^{k,v}$ represent the errors in the channel estimates corresponding to the lth path between the ith transmit antenna $(i = 1, 2)$ and the vth receive antenna. From (6), we obtain the corresponding channel estimates as

$$\begin{aligned} \hat{h}_{1l}^{k,v} &= h_{1l}^{k,v} + e_{1l}^{k,v} \\ \hat{h}_{2l}^{k,v} &= h_{2l}^{k,v} + e_{2l}^{k,v}, \qquad k = 1, 2, \ldots, K \quad l = 1, 2, \ldots, L \end{aligned} \tag{7}$$

where $e_{il}^{k,v} = (w_{il}^{k,v}/B)$ $(i = 1, 2)$. It is noted that the errors in channel estimates at the vth receive antenna $e_{il}^{k,v} (i = 1, 2; l = 1, \ldots, L; k = 1, \ldots, K)$ are modeled as complex Gaussian variables with zero mean and covariance matrix $\mathbf{R}_{E-E}$ (see Appendix B).

IV. Data Detection

Having obtained the channel estimates as discussed in the previous section and prior to data detection, the effect of the pilot sequences at each receive antenna is eliminated from the sampled received signal as follows. Similar to the channel estimation procedure, $r^v(t)$ is filtered, sampled at a rate $1/T_c$, and accumulated over an observation interval of $(2N + \tau_{\max} + L - 1)$ chips for the mth data symbol of the received data block. Then, using the reconstructed samples of the pilot signals, with the aid of channel estimates, we can exclude the interference effect of the pilot signals on each data estimation interval. From Fig. 2, the data chip-matched filter output after suppressing the effect of pilot sequences at the vth receive antenna $\mathbf{g}^v[m]$ can be expressed as

$$\begin{aligned} \mathbf{g}^v[0] = {} & \mathbf{C}'[0]\mathbf{H}^{v'}\mathbf{b}'[0] + \mathbf{C}'[1]\mathbf{H}^{v'}\mathbf{b}'[1] - \mathbf{P}[0]\mathbf{E}^{v'} \\ & - \mathbf{P}[1]\mathbf{E}^{v'} + \mathbf{n}^v[0], \end{aligned} \tag{8}$$

$$\begin{aligned} \mathbf{g}^v[m] = {} & \mathbf{C}'[0]\mathbf{H}^{v'}\mathbf{b}'[m] + \mathbf{C}'[-1]\mathbf{H}^{v'}\mathbf{b}'[m-1] \\ & + \mathbf{C}'[1]\mathbf{H}^{v'}\mathbf{b}'[m+1] - \mathbf{P}[0]\mathbf{E}^{v'} - \mathbf{P}[-1]\mathbf{E}^{v'} \\ & - \mathbf{P}[1]\mathbf{E}^{v'} + \mathbf{n}^v[m], m = 1, \ldots, M-2 \end{aligned} \tag{9}$$

$$\begin{aligned} \mathbf{g}^v[M-1] = {} & \mathbf{C}'[0]\mathbf{H}^{v'}\mathbf{b}'[M-1] + \mathbf{C}'[-1]\mathbf{H}^{v'}\mathbf{b}'[M-2] \\ & - \mathbf{P}[0]\mathbf{E}^{v'} - \mathbf{P}[-1]\mathbf{E}^{v'} + \mathbf{n}^v[M-1] \end{aligned} \tag{10}$$

where $\mathbf{C}'[0]$, $\mathbf{C}'[1]$, and $\mathbf{C}'[-1]$ include the data sequences corresponding to the current, following, and previous STS symbols of the K-user system within the observation interval, respectively, each having a dimension of $(2N + L - 1 + \tau_{\max}) \times 2LK$ (see Appendix A). Similarly, $\mathbf{P}[0]$, $\mathbf{P}[1]$, and $\mathbf{P}[-1]$ have the same definitions of $\mathbf{C}'[0]$, $\mathbf{C}'[1]$, and $\mathbf{C}'[-1]$, except that the data sequences are replaced by the pilot sequences. In (8)–(10), the channel impulse response of the K users $\mathbf{H}^{v'}$ is defined by

$$\mathbf{H}^{v'} = \operatorname{diag}\left\{\mathbf{H}_1^{v'}, \mathbf{H}_2^{v'}, \ldots, \mathbf{H}_K^{v'}\right\}$$

where

$$\mathbf{H}_k^{v'} = \left[\mathbf{H}_k^{v'T}(1), \mathbf{H}_k^{v'T}(2), \ldots, \mathbf{H}_k^{v'T}(L)\right]^T \qquad k = 1, 2, \ldots, K.$$

$\mathbf{H}_k^{v'}(l)$ $(l = 1, \ldots, L)$ is defined according to the employed STS scheme in [8] as

$$\mathbf{H}_k^{v'}(l) = \begin{bmatrix} h_{1l}^{k,v} & h_{2l}^{k,v} \\ -h_{2l}^{k,v} & h_{1l}^{k,v} \end{bmatrix}.$$

In (8), $\mathbf{E}^{v'}$ represents the channel estimation error vector of the K users, which is given by

$$\mathbf{E}^{v'} = \left[\mathbf{E}_1^{v'T}, \mathbf{E}_2^{v'T}, \ldots, \mathbf{E}_K^{v'T}\right]^T$$

where

$$\mathbf{E}_k^{v'} = \left[e_{11}^{k,v}, e_{21}^{k,v}, e_{12}^{k,v}, \ldots, e_{1L}^{k,v}, e_{2L}^{k,v}\right]^T, \qquad k = 1, 2, \ldots, K.$$

Finally, in (10), $\mathbf{b}'[m]$ $(m = 0, \ldots, M-1)$ is given by

$$\mathbf{b}'[m] = \left[\mathbf{b}_1'^T[m], \mathbf{b}_2'^T[m], \ldots, \mathbf{b}_K'^T[m]\right]^T$$

where

$$\mathbf{b}_k'[m] = [Ab_{k1}[m], Ab_{k2}[m]]^T \qquad k = 1, 2, \ldots, K \quad m = 0, \ldots, M-1$$

where $A = \sqrt{(\rho_d/2)}$. From (8)–(10), the received signal can be represented in a more compact form as

$$\mathbf{g}^v[m] = \mathbf{C}_d\mathbf{H}_d^v\mathbf{b}_d - B\mathbf{P}_p\mathbf{E}^v + \mathbf{n}^v[m] \qquad m = 1, \ldots, M-2 \tag{11}$$

where

$$\mathbf{C}_d = [\mathbf{C}'[0], \mathbf{C}'[-1], \mathbf{C}'[1]] \tag{12}$$

$$\mathbf{P}_p = [\mathbf{P}[0], \mathbf{P}[-1], \mathbf{P}[1]] \tag{13}$$

$$\mathbf{H}_d^v = \mathbf{I}_3 \otimes \mathbf{H}^{v'} \tag{14}$$

$$\mathbf{E}^v = \left[\mathbf{E}^{v'^T}, \mathbf{E}^{v'^T}, \mathbf{E}^{v'^T}\right]^T \tag{15}$$

$$\mathbf{b}_d = \left[\mathbf{b}'[m]^T, \mathbf{b}'[m-1]^T, \mathbf{b}'[m+1]^T\right]^T. \tag{16}$$

Note that in the case of $m = 0$, one can exclude, from (12)–(16), the effect of previous STS symbols on the data chip-matched filter output $\mathbf{g}^v[m]$. Furthermore, when $m = M-1$, the effect of following symbols are excluded. After sampling the received signal, the data-matched filter output $\mathbf{g}^v[m]$ $(v = 1, \ldots, V)$ is correlated with the data code matrix $\mathbf{C}_d$ as follows:

$$\mathbf{g}_c^v[m] = \mathbf{R}_d \mathbf{H}_d^v \mathbf{b}_d - B\mathbf{C}_d^H \mathbf{P}_p \mathbf{E}^v + \mathbf{N}_{dc}^v[m] \tag{17}$$

where $\mathbf{R}_d = \mathbf{C}_d^H \mathbf{C}_d$ represents the data cross-correlation matrix, and $\mathbf{N}_{dc}^v[m]$ is modeled as $N_c(\mathbf{0}, \mathbf{R}_d)$. It is clear from (17) that the data correlator output $\mathbf{g}_c^v[m]$ suffers from MAI and ISI. Afterward, the output of the data correlator (despreader) at each receive antenna is applied to a linear mapper defined by the inverse of the cross-correlation matrix $\mathbf{R}_d^{-1}$ corresponding to the data code sequences to give

$$\mathbf{g}_d^v[m] = \mathbf{H}_d^v \mathbf{b}_d - B\mathbf{Q}_d \mathbf{E}^v + \mathbf{N}_{dd}^v[m] \tag{18}$$

where $\mathbf{Q}_d = \mathbf{R}_d^{-1}\mathbf{C}_d^H \mathbf{P}_p$, and $\mathbf{N}_{dd}^v[m]$ is modeled as $N_c(\mathbf{0}, \mathbf{R}_d^{-H})$. Finally, the first $2LK$ elements of each decorrelator output vector $\mathbf{g}_d^v[m](v = 1, \ldots, V)$ are combined with the corresponding channel estimates defined in (7) for final data estimates. Without loss of generality, we consider the first user as the desired user. Thus, the decision variables for the odd and even data bits are given by

$$\hat{b}_{11}[m] = \sum_{v=1}^{V}\sum_{l=1}^{L} Re\left\{\hat{h}_{1l}^{1,v*}\left(\mathbf{g}_d^v[m]\right)_{2l-1,1} - \hat{h}_{2l}^{1,v*}\left(\mathbf{g}_d^v[m]\right)_{2l,1}\right\} \tag{19}$$

$$\hat{b}_{12}[m] = \sum_{v=1}^{V}\sum_{l=1}^{L} Re\left\{\hat{h}_{2l}^{1,v*}\left(\mathbf{g}_d^v[m]\right)_{2l-1,1} + \hat{h}_{1l}^{1,v*}\left(\mathbf{g}_d^v[m]\right)_{2l,1}\right\} \tag{20}$$

where $(\mathbf{g}_d^v[m])_{\delta,1}$ $(\delta = 1, 2, \ldots, UL)$ is the δth element of the vth decorrelator output vector, and $Re\{\cdot\}$ denotes real-part operation.

In the aforementioned analysis, we have considered the case of two transmit antennas. However, the estimation technique can be generalized to the case of $U \geq 2$ transmit antennas as follows. The transmitted data are first serial-to-parallel converted to U parallel substreams. As in the two-transmit-antenna case, the U parallel bits are spread using the STS scheme in [8]. Following the STS, the U parallel data bits are superimposed by U distinct pilot spreading codes, where each pilot sequence is assigned to a different antenna. Upon reception, the received signal is sampled at the chip rate and accumulated over an estimation interval of $UN + L - 1 + \tau_{\max}$, where L is the number of resolvable paths, and $\tau_{\max}$ is the user's delay spread. Following the same procedure as in the two-antenna case, the received signal after sampling is despread using $\mathbf{C}_p$ for channel estimation or $\mathbf{C}_d$ for data detection. Subsequently, decorrelation is implemented to remove the effect of MAI and ISI from both channel and data estimates.

V. Performance Analysis

In this section, we evaluate the performance of the proposed estimation technique in terms of its probability of bit error. We start by finding the decision variables corresponding to the data estimates at the decorrelator output and after signal combining. Then, we obtain the pdf of these decision variables, which will facilitate the evaluation of the average probability of error.

A. BER Analysis

From (18), $(\mathbf{g}_d^v[m])_{2l-1,1}$ and $(\mathbf{g}_d^v[m])_{2l,1}$ in (19) and (20) are given by

$$\left(\mathbf{g}_d^v[m]\right)_{2l-1,1} = Ah_{1l}^{1,v} b_{11}[m] + Ah_{2l}^{1,v} b_{12}[m] - B \times \left(\mathbf{Q}_d \mathbf{E}^v\right)_{2l-1,1} + \left(\mathbf{N}_{dd}^v\right)_{2l-1,1} \tag{21}$$

$$\left(\mathbf{g}_d^v[m]\right)_{2l,1} = -Ah_{2l}^{1,v} b_{11}[m] + Ah_{1l}^{1,v} b_{12}[m] - B \times \left(\mathbf{Q}_d \mathbf{E}^v\right)_{2l,1} + \left(\mathbf{N}_{dd}^v\right)_{2l,1} \tag{22}$$

where $(\mathbf{Q}_d\mathbf{E}^v)_{2l-1,1}$ and $(\mathbf{Q}_d\mathbf{E}^v)_{2l,1}$ are defined in terms of the channel-estimation errors corresponding to the K users at the vth receive antenna. By partitioning $\mathbf{Q}_d$ into three groups, i.e., $\mathbf{Q}_{d1}$, $\mathbf{Q}_{d2}$, and $\mathbf{Q}_{d3}$, where each group has the same dimensions of $6LK \times 2LK$, $\mathbf{Q}_d\mathbf{E}^v$ is defined as $\mathbf{Q}_{ds}\mathbf{E}^{v'}$, where $\mathbf{Q}_{ds} = \mathbf{Q}_{d1} + \mathbf{Q}_{d2} + \mathbf{Q}_{d3}$. Consequently, $(\mathbf{Q}_d\mathbf{E}^v)_{2l-1,1}$ and $(\mathbf{Q}_d\mathbf{E}^v)_{2l,1}$ are derived as

$$\left(\mathbf{Q}_d \mathbf{E}^v\right)_{2l-1,1} = \mathbf{X}_{2l-1}\mathbf{E}^{v'} \tag{23}$$

$$\left(\mathbf{Q}_d \mathbf{E}^v\right)_{2l,1} = \mathbf{X}_{2l}\mathbf{E}^{v'} \tag{24}$$

where $\mathbf{X}_f (f = 2l-1, 2l)$ is a $[1 \times 2LK]$ vector consisting of the elements of the fth raw of $\mathbf{Q}_{ds}$. Using (7) and (21)–(24), (19) can be written as

$$\begin{aligned}
\hat{b}_{11}[m] =& \sum_{v=1}^{V}\sum_{l=1}^{L} Re \times \left\{\left(A\left|h_{1l}^{1,v}\right|^2 + A\left|h_{2l}^{1,v}\right|^2 + Ae_{1l}^{1v*}h_{1l}^{1,v} + Ae_{2l}^{1,v*}h_{2l}^{1,v}\right)b_{11}[m]\right. \\
&+\left(Ae_{1l}^{1,v*}h_{2l}^{1,v} - Ae_{2l}^{1,v*}h_{1l}^{1,v}\right)b_{12}[m] - Bh_{1l}^{1,v*}\mathbf{X}_{2l-1}\mathbf{E}^{v'} \\
&- Be_{1l}^{1,v*}\mathbf{X}_{2l-1}\mathbf{E}^{v'} + Bh_{2l}^{1,v*}\mathbf{X}_{2l}\mathbf{E}^{v'} + Be_{2l}^{1,v*}\mathbf{X}_{2l}\mathbf{E}^{v'} \\
&+ h_{1l}^{1,v*}\left(\mathbf{N}_{dd}^v\right)_{2l-1,1} + e_{1l}^{1,v*}\left(\mathbf{N}_{dd}^v\right)_{2l-1,1} - h_{2l}^{1,v*}\left(\mathbf{N}_{dd}^v\right)_{2l,1} \\
&\left. - e_{2l}^{1,v*}\left(\mathbf{N}_{dd}^v\right)_{2l,1}\right\}.
\end{aligned} \tag{25}$$

Now, consider the case of $b_{11}[m] = +1$; then, the probability of error is given by

$$P_b = \frac{1}{2}P\left(\hat{b}_{11}[m] < 0 | b_{12}[m] = +1\right) + \frac{1}{2}P\left(\hat{b}_{11}[m] < 0 | b_{12}[m] = -1\right). \quad (26)$$

Let the estimate $\hat{b}_{11}[m]$ be equivalent to Z_1 when $b_{12}[m] = +1$ and Z_2 when $b_{12}[m] = -1$. Then, (26) can be written as

$$P_b = \frac{1}{2}P_b(Z_1 < 0) + \frac{1}{2}P_b(Z_2 < 0). \quad (27)$$

Given the complex variables x and y, we have

$$Re\{xy^*\} = \frac{1}{2}(xy^* + yx^*). \quad (28)$$

Then, Z_1 and Z_2 can be expressed as a sum of independent symmetric quadratic forms as follows:

$$Z_1 = \sum_{v=1}^{V} \mathbf{X}^{vH}\mathbf{S}_1\mathbf{X}^v = \sum_{v=1}^{V} Z_{1v} \quad (29)$$

$$Z_2 = \sum_{v=1}^{V} \mathbf{X}^{vH}\mathbf{S}_2\mathbf{X}^v = \sum_{v=1}^{V} Z_{2v} \quad (30)$$

where

$$\mathbf{X}^v = \Big[h_{11}^{1,v}, h_{21}^{1,v}, h_{12}^{1,v}, \ldots, h_{2L}^{1,v}, e_{11}^{1,v}, e_{21}^{1,v}, \ldots, e_{2L}^{1,v}, \ldots, e_{2L}^{K,v}, (\mathbf{N}_{dd}^v)_{1,1}, (\mathbf{N}_{dd}^v)_{2,1}, \ldots, (\mathbf{N}_{dd}^v)_{2L-1,1}, (\mathbf{N}_{dd}^v)_{2L,1}\Big]^T \quad (31)$$

and $\mathbf{S}_1$ and $\mathbf{S}_2$ are coefficient matrices defined in Appendix C. It should be noted that $\mathbf{X}^v$ is a $[4L + 2LK]$ complex normal vector with zero mean and covariance matrix $\mathbf{R}$ (the derivation of $\mathbf{R}$ is defined in Appendix B). The vectors $\mathbf{X}^v (v = 1, \ldots, V)$ are statistically independent with the same covariance matrix $\mathbf{R}$. Furthermore, the coefficient matrices $\mathbf{S}_1$ and $\mathbf{S}_2$ are identical for each receive antenna. In our system model, we assume that there is enough spacing between the receive antenna elements such that the channel coefficients, the errors in channel estimates, and the noise samples at each receive antenna (i.e., the parameters of $\mathbf{X}^v$, $v = 1, \ldots, V$) can be assumed to be statistically independent [22]. Therefore, $\mathbf{Z}_{1v}$, $v = 1, \ldots, V$, are assumed to be independent.

From (29), we can find the characteristic function of the decision statistic Z_1 as [23], [24]

$$\Phi_{Z_1}(\omega) = E\left[\exp[j\omega Z_1]\right] = E\left[\exp\left(j\omega \sum_{v=1}^{V} Z_{1v}\right)\right] = \prod_{v=1}^{V} \phi_{Z_{1v}}(\omega) \quad (32)$$

where

$$\phi_{Z_{1v}}(\omega) = E\left[\exp(j\omega Z_{1v})\right] \quad (33)$$

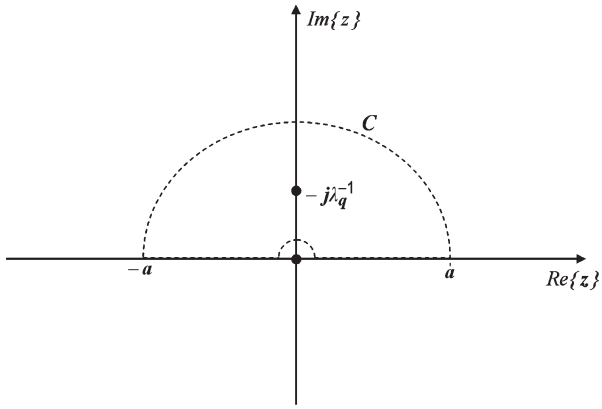

Fig. 3. Indented contour C.

and $E[\cdot]$ denotes statistical expectation. Note that the characteristic function of the quadratic form in (33) can be derived in terms of the eigenvalues of the matrix $\mathbf{S}_1\mathbf{R}$ as [24]

$$\phi_{Z_{1v}}(\omega) = \prod_{n=1}^{N} \frac{1}{(1 - j\omega\lambda_n)} \quad (34)$$

where λ_n, $n = 1, \ldots, N$ are the N eigenvalues of the $\mathbf{S}_1\mathbf{R}$ matrix. Based on the matrix structure of $\mathbf{S}_1$ and $\mathbf{R}$ (see Appendices B and C), both $\mathbf{S}_1$ and $\mathbf{R}$ are symmetric matrices. Furthermore, we can notice that $\mathbf{R}$ is positive definite, while $\mathbf{S}_1$ is generally a singular matrix. Accordingly, the eigenvalues λ_n, $n = 1, \ldots, N$, are real valued but may be positive or negative. Substituting (34) in (32), the characteristic function $\Phi_{Z_1}(\omega)$ is given by

$$\Phi_{Z_1}(\omega) = \prod_{n=1}^{N} \frac{1}{(1 - j\omega\lambda_n)^V}. \quad (35)$$

From (35), we can find the pdf of Z_1, i.e., f_{Z_1} [25]. Using this pdf, one can evaluate the probability $P_b(Z_1 < 0)$ as follows [26]:

$$\begin{aligned} P_b(Z_1 < 0) &= \int_{-\infty}^{0} f_{Z_1} dZ_1 \\ &= \frac{1}{2\pi}\int_{-\infty}^{0}\int_{-\infty}^{\infty} \Phi_{Z_1}(\omega)\exp[-j\omega Z_1]d\omega dZ_1 \\ &= \frac{1}{2} - \frac{1}{2\pi}\int_{-\infty}^{\infty}\left[\prod_{n=1}^{N}\frac{1}{(1 - j\omega\lambda_n)^V}\right](j\omega)^{-1}d\omega. \end{aligned} \quad (36)$$

The remaining integral in (36) can be evaluated using contour integration, where we consider the integral along an indented contour C oriented in the positive direction, as shown in Fig. 3. The contour integral is then given by

$$\oint_C f(z)dz = \oint_C \left[\prod_{n=1}^{N}\frac{1}{(1 - jz\lambda_n)^V}\right](jz)^{-1}dz. \quad (37)$$

Note that the integrand in (37) has singularities at $z = 0$ and $z = -j/\lambda_1, \ldots, -j/\lambda_N$. Since the contour C is located in the upper half-plane, the poles bounded by this contour are based on the negative eigenvalues (i.e., $\{\lambda_n\} < 0$). Using the residue theorem [27], the contour integral defined in (37) is given by

$$\oint_C f(z)dz = j\pi Res\left(f(z), z = 0\right) + j2\pi \sum_{q=1}^{n_1} Res\left(f(z), z = -\frac{j}{\lambda_q}\right) \quad (38)$$

where $Res(f(z), z_o)$ denotes the residue of $f(z)$ at the pole $z = z_o$, and n_1 represents the number of negative eigenvalues of the matrix $\mathbf{S_1R}$. To evaluate the residues, we use the partial fraction expansion method of a rational function with high-order poles. For further details regarding this method, see [28]. In (38), for all values of V, we have

$$Res\left(f(z), z = 0\right) = -j. \quad (39)$$

For the remaining distinct poles, the residues are found for different values of V according to [28]. For instance, for $V = 1,\ 2,$ and 3 receive antennas, we have, respectively, the following cases.

Case 1) $(V = 1)$

$$Res\left(f(z), z = -\frac{j}{\lambda_q}\right) = \prod_{q'=1, \lambda_{q'} \neq \lambda_q}^{N} \frac{j}{\left(1 - \frac{\lambda'_q}{\lambda_q}\right)}. \quad (40)$$

Case 2) $(V = 2)$

$$Res\left(f(z), z = -\frac{j}{\lambda_q}\right) = j\lambda_q \cdot \prod_{n=1, \lambda_n \neq 0}^{N} \lambda_n^{-2} \cdot \prod_{q'=1, \lambda_{q'} \neq \lambda_q}^{N} \times \left(\frac{1}{\left(\lambda_{q'}^{-1} - \lambda_q^{-1}\right)^2} \cdot \left[\lambda_q - \sum_{q'=1, \lambda_{q'} \neq \lambda_q}^{N} \frac{2}{\lambda_{q'}^{-1} - \lambda_q^{-1}} \right] \right). \quad (41)$$

Case 3) $(V = 3)$

$$Res\left(f(z), z = -\frac{j}{\lambda_q}\right) = \frac{j\lambda_q}{2} \cdot \prod_{n=1, \lambda_n \neq 0}^{N} \lambda_n^{-3} \cdot \prod_{q'=1, \lambda_{q'} \neq \lambda_q}^{N} \times \left(\frac{1}{(\lambda_{q'}^{-1} - \lambda_q^{-1})^3} \cdot \left[\lambda_q^2 + \sum_{q'=1, \lambda_{q'} \neq \lambda_q}^{N} \frac{3}{\left(\lambda_{q'}^{-1} - \lambda_q^{-1}\right)^2} + \left(\lambda_q - \sum_{q'=1, \lambda_{q'} \neq \lambda_q}^{N} \frac{3}{\lambda_{q'}^{-1} - \lambda_q^{-1}} \right)^2 \right] \right). \quad (42)$$

Now, using the obtained residues, we can evaluate the contour integral in (38). Note that the contour C can be split into a straight part (real part) and a curved part. Let $f(z) = P(z)/Q(z)$, where the degrees of $P(z)$ and $Q(z)$ are u and s, respectively; then, the integration over the curved path tends to zero for a large $|z|(|z| \to \infty)$ when $s \geq u + 2$ [27, Th. (19.5)]. Given this fact and considering the limit as a goes to infinity, the integration defined in (38) can be evaluated as

$$\int_{-\infty}^{\infty} f(\omega)d\omega = j\pi Res\left(f(z), z = 0\right) + j2\pi \sum_{q=1}^{n_1} Res\left(f(z), z = -\frac{j}{\lambda_q}\right) \quad (43)$$

where a represents the radius of the contour C, and ω denotes the real part of the complex variable z. Substituting (43) in (36), we get $P_b(Z_1 < 0)$ for the cases with $V = 1, 2,$ and 3 antennas, respectively, as follows.

Case 1) $(V = 1)$

$$P_b(Z_1 < 0) = \left(\prod_{n=1, \lambda_n \neq 0}^{N} \lambda_n^{-1} \right) \cdot \sum_{q=1}^{n_1} \left(\lambda_q \prod_{q'=1, \lambda_{q'} \neq \lambda_q}^{N} \frac{1}{\left(\lambda_{q'}^{-1} - \lambda_q^{-1}\right)} \right). \quad (44)$$

Case 2) $(V = 2)$

$$P_b(Z_1 < 0) = \left(\prod_{n=1, \lambda_n \neq 0}^{N} \lambda_n^{-2} \right) \cdot \sum_{q=1}^{n_1} \left(\lambda_q \prod_{q'=1, \lambda_{q'} \neq \lambda_q}^{N} \frac{1}{\left(\lambda_{q'}^{-1} - \lambda_q^{-1}\right)^2} \cdot \left[\lambda_q - \sum_{q'=1, \lambda_{q'} \neq \lambda_q}^{N} \frac{2}{\lambda_{q'}^{-1} - \lambda_q^{-1}} \right] \right). \quad (45)$$

Case 3) $(V = 3)$

$$P_b(Z_1 < 0) = \left(\prod_{n=1, \lambda_n \neq 0}^{N} \lambda_n^{-3} \right) \cdot \sum_{q=1}^{n_1} \times \left(\frac{\lambda_q}{2} \cdot \prod_{q'=1, \lambda_{q'} \neq \lambda_q}^{N} \frac{1}{\left(\lambda_{q'}^{-1} - \lambda_q^{-1}\right)^3} \cdot \left[\lambda_q^2 + \sum_{q'=1, \lambda_{q'} \neq \lambda_q}^{N} \frac{3}{\left(\lambda_{q'}^{-1} - \lambda_q^{-1}\right)^2} + \left(\lambda_q - \sum_{q'=1, \lambda_{q'} \neq \lambda_q}^{N} \frac{3}{\lambda_{q'}^{-1} - \lambda_q^{-1}} \right)^2 \right] \right). \quad (46)$$

Following the same procedure, we can evaluate the probability $P_b(Z_2 < 0)$ by replacing λ_n by β_n and n_1 by n_2, where β_n, $n = 1, \ldots, N$ are the eigenvalues of $\mathbf{S}_2\mathbf{R}$, and n_2 is the number of the corresponding negative eigenvalues. Finally, the average BER in (27) is obtained.

In the aforementioned analysis, we considered a uniform multipath intensity profile (MIP). However, this analysis can be generalized to the exponential MIP in the same manner where the subscript l is added to the corresponding variance of each multipath component, i.e., σ_h^2 is replaced by σ_{hl}^2, $l = 1, \ldots, L$, where σ_{hl}^2 is defined by [29]

$$\sigma_{hl}^2 = \sigma_o^2 \exp\left(-\frac{\delta(l-1)}{L}\right), \qquad l = 1, \ldots, L \tag{47}$$

σ_o^2 is the average power of the initial path, and δ is the normalized decay factor. To keep the total fading power equal to unity at each transmit antenna, we have

$$\sigma_o^2 = \frac{\exp\left(-\frac{\delta}{L}\right) - 1}{\exp(-\delta) - 1}. \tag{48}$$

Thus, the covariance of the channel vector $\mathbf{h}^v$, i.e., $\mathbf{R}_{H-H}$, is defined by a diagonal matrix with elements $\sigma_{h1}^2, \sigma_{h2}^2, \ldots, \sigma_{hL}^2$ (see Appendix B). Based on these assumptions and following the same procedure mentioned previously, the closed forms of the average BER will have the same expressions as in (51)–(53), which is shown later, regardless of the channel power delay profile.

B. Asymptotic Performance and Diversity

One way to prove that our system can deliver the full system diversity is through a comparison with the corresponding maximal-ratio combiner (MRC) with the same number of diversity branches. In that, we show that the slope of the BER performance for the two systems at a high SNR is identical, indicating equal diversity orders. This approach is investigated in more details in the following section. On the other hand, if the eigenvalues of the matrix $\mathbf{S}_1\mathbf{R}$ of each receive antenna can be evaluated in terms of the received signal parameters, then (44)–(46) can also be used to provide further insight into the proposed system performance. Unfortunately, a straightforward application of this approach proved to be intractable as the dimension of the corresponding matrix is $(4L + 2LK) \times (4L + 2LK)$.

In [30], Russ and Varanasi have encountered a similar problem when dealing with noncoherent multiuser detection over Rayleigh fading channels. Similarly, Brehler and Varanasi [31] have noticed the same problem in analyzing the performance of quadratic receivers in fading channels. In these works, the authors have presented the BER performance of their receivers as a function of the eigenvalues of some parametric matrices. A remedy to this problem was proposed in [30] and [31], where the authors examined the asymptotic behavior of the corresponding eigenvalues as the SNR increases ($\rho_d \to \infty$). Using empirical results, the authors in [31] observed that half of the nonzero eigenvalues asymptotically approach -1, while the other half are positive and linearly proportional to ρ_d. As a result, they concluded that such a structure of eigenvalues is sufficient to prove the full system diversity is equal to the number of asymptotic positive (negative) eigenvalues.

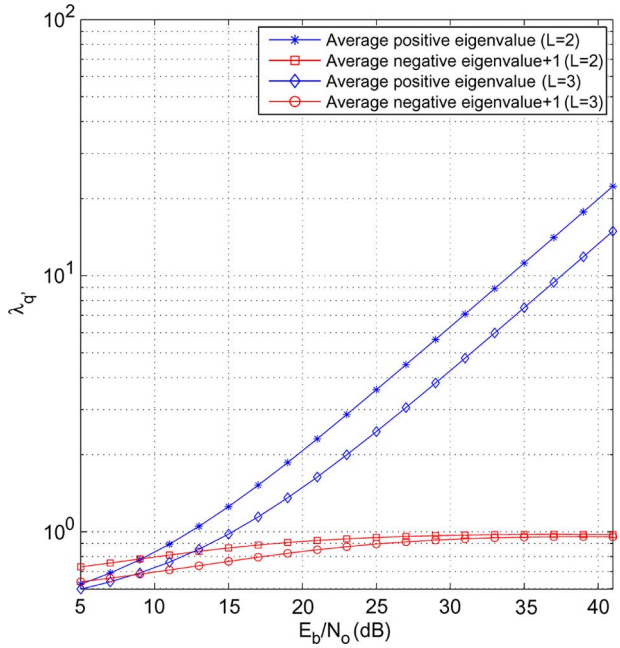

Fig. 4. Asymptotic nonzero eigenvalues of a five-user STS system with $L = 2$ and 3 paths, PNR $= 5$ dB, two antennas at the transmitter, and one antenna at the receiver side.

In the previous section, we have shown that $\mathbf{S}_1\mathbf{R}$ is defined for any vth receive antenna $v = 1, \ldots, V$ (see also Appendices B and C). Therefore, the estimated eigenvalues of this matrix are equivalent to the eigenvalues of an STS system with two transmit antennas and one receive antenna assuming L resolvable paths per transmit antenna (equivalent to a system with $2L$ diversity order).

Following the same approach as in [30] and [31], we have noticed that half of the nonzero eigenvalues are asymptotically equal to ϵ ($\epsilon \to 0^-$ as the SNR $\rho_d \to \infty$), where 0^- denotes a very small negative value. The remaining half of the nonzero asymptotic eigenvalues is positive and linearly proportional to ρ_d. It should be noted, however, that this result did not turn out to be identical to the result obtained in [31] since we consider a different system configuration. Similarly, the structure of these eigenvalues show that the number of asymptotic positive (negative) eigenvalues is equivalent to the full diversity of an STS system with $2L$ diversity order. Fig. 4 shows a sample of our results where we consider the proposed system with five users, two transmit antennas, and one receive antenna for $L = 2$ and 3 resolvable paths. This system produces a group of eight nonzero eigenvalues for the first case ($L = 2$) and a group of 12 nonzero eigenvalues for the second case ($L = 3$). For each group, half of the nonzero eigenvalues are positive, and the other half are negative. This confirms that the number of positive eigenvalues represents the full system diversity, where the number of positive eigenvalues of each group (four and six, respectively) is equal to the full system diversity of each case.

By utilizing this asymptotic behavior of eigenvalues, we are able to study the behavior of the BER as $\rho_d \to \infty$. Note that the first term in the right-hand side of (44)–(46) takes the form $\prod_{n=1,\lambda_n\neq 0}^{N} \lambda_n^{-V}$, where $V = 1, 2$, and 3 receive antennas. In the asymptotic case, this term is proportional to ρ_d^{-2LV}. The remaining terms that belong to the right-hand side of these equations include a common factor in the form

$$\left(\prod_{q'=1,\lambda_{q'}\neq\lambda_q}^{N} \frac{1}{\left(\lambda_{q'}^{-1} - \lambda_q^{-1}\right)^V} = \prod_{q'=1,\lambda_{q'}\neq\lambda_q}^{N} \frac{\lambda_q^V}{\left(\frac{\lambda_q}{\lambda_{q'}} - 1\right)^V} \right) \qquad V = 1, 2, 3.$$

Taking the limit of this term as $\rho_d \to \infty$ and substituting with the positive and negative asymptotic eigenvalues, one can easily show that the limit of this term has a constant value independent of the SNR ρ_d. Consequently, using this intuitive approach, the BER expressions in (44)–(46) show that the proposed system achieves a diversity order of $2LV$.

VI. Simulation Results

Here, we examine the BER performance of the STS system employing the proposed $\mathbf{S}_1$ and data-estimation technique. Both Monte Carlo simulations and the analytical results are presented for different system configurations. In all cases, we consider a DS-CDMA system with two transmit and $V = 1,\ 2,$ and 3 receive antennas. We also consider an uplink asynchronous transmission of a data block of $M = 1000$ bits over a frequency-selective slow-fading channel. Throughout the simulations, we consider a multiuser system where all users are assigned Walsh code sequences of length 64 chips for the pilot and data sequences. The delays among user signals $(\tau_k, k \in \{1, 2, \ldots, K\})$ are assumed to be a multiple of chip periods within T_s. Without loss of generality, we assume that the users' delays satisfy the condition $\tau_1 = 0 \leq \cdots \leq \tau_k \leq \cdots \leq \tau_K \leq T_s$ [17]. The path delay is also assumed to be a multiple of chip intervals $\tilde{\tau}_l = lT_c, l = 1, 2, \ldots, L$. We assume that the channel coefficients are fixed for the duration of one data frame where the pilot sequence is superimposed to the STS signal during the first symbol. In the simulations, we investigate the BER performance of the STS system versus different total signal-power-(data and pilot)-to-noise ratios Eb/No.

Fig. 5 shows the BER performance for different channel estimation and data detection techniques: 1) perfect knowledge of the channel at the receiver (reference case); 2) conventional channel estimation and data detection [16] (no MAI removal from both the channel and data estimates); 3) conventional channel estimation followed by decorrelating data detection (only interference removal from the data estimates); and 4) the proposed decorrelating channel- and data-estimation technique. Confirmed by simulations, our analytical results prove that the proposed scheme achieves performance very close to the perfect channel-estimation case for an average pilot-power-to-noise ratio PNR $= 5$ dB. Examining the results in Fig. 5, one can see the effect of interference removal from both channel and data estimates on the system performance. Note that the third system renders a slight improvement over the conventional technique [16], due to the MAI removal from the data estimates but still affected by the imperfect channel estimation. With MAI removal from both the channel and data estimates, the proposed receiver outperforms the other estimation techniques. For reference, we included the BER performance of the MRC with four diversity branches. We can notice that the proposed scheme is able to deliver the full system diversity $(2VL)$ at the prescribed PNR.

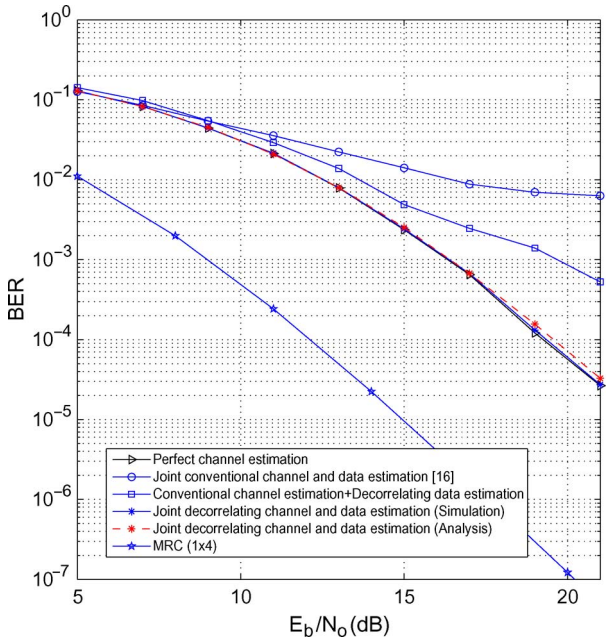

Fig. 5. Comparison between different $\mathbf{S}_1$ estimation and data-detection techniques for the five-user STS system with $L = 2$ paths, PNR $= 5$ dB, two antennas at the transmitter, and one antenna at the receiver side.

Fig. 6 shows the performance of the proposed system with the same antenna configuration as a function of the PNR. Compared with the perfect channel-estimation case, the proposed receiver achieves accurate estimates for a PNR greater than 0 dB. In Fig. 7, the BER performance of our system is examined for 2×3 MIMO systems with two resolvable paths per transmit antenna and a different numbers of users. The results conclude that the effect of increased interference only appears as an SNR loss, and no diversity loss is incurred.

In Fig. 8, we investigate the performance of our proposed system considering different channel power delay profiles, namely, uniform MIP with unity total fade power $(\sigma_h^2 = 1/L)$ and exponential MIP with unity total fade power [see (47)]. The results show that the realistic channel assumptions are interpreted as SNR loss without affecting the full system diversity.

In all the results, our analytical results are shown to be in excellent agreement with the simulated ones, and the full system diversity is maintained.

As a final note on the performance of superimposed pilot (SIP) versus conventional time-multiplexed pilot (CP) schemes, Coldrey and Bohlin [32] provide a comparative study between these two schemes for MIMO systems using the capacity as a performance measure. According to their investigation, SIP achieves a higher capacity in particular scenarios such as many

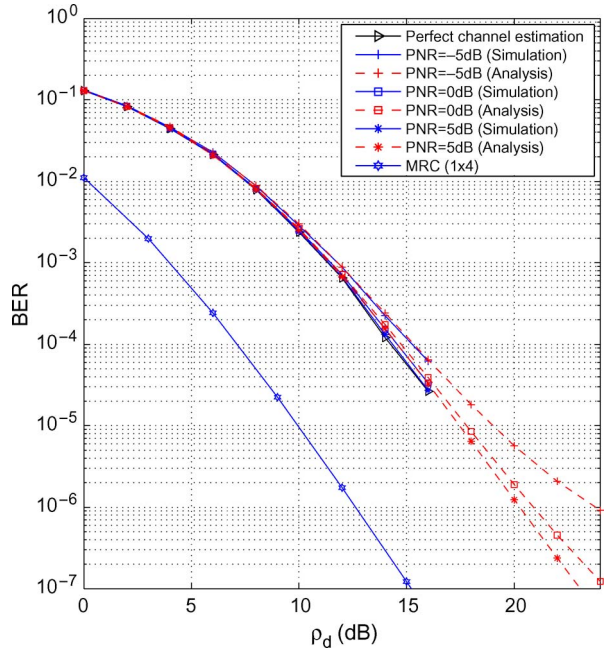

Fig. 6. Effect of different PNR values on the BER performance of the proposed estimation technique for a five-user STS system with $L = 2$ paths, two antennas at the transmitter, and one antenna at the receiver side.

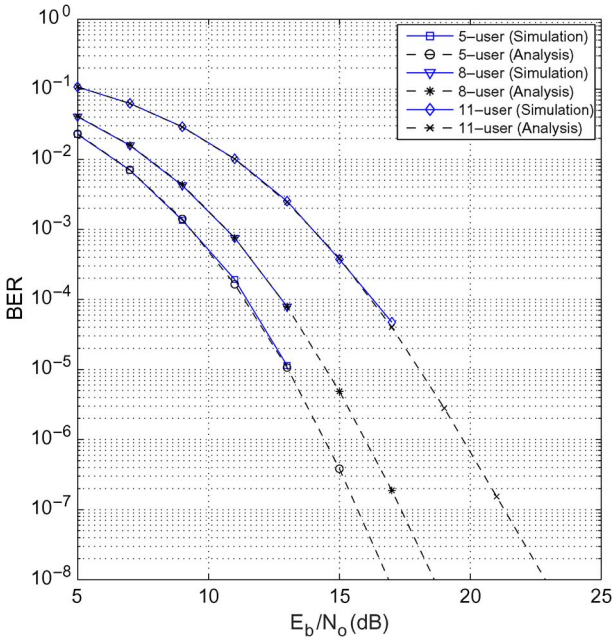

Fig. 7. BER performance of the proposed estimation technique for the multi-user STS system with $L = 2$ paths and PNR $= 5$ dB. The STS system employs two transmit antennas and $V = 3$ antennas at the receiver side.

receive antennas and/or short channel coherence times. However, in other scenarios, the quality of the channel estimates produced by the SIP scheme is degraded due to the presence of unknown data during channel estimation. This, as stated in [32], deteriorates the information throughput and degrades its gain over the CP scheme. In other words, the main drawback of SIP is the poor channel estimation due to the interference of the transmitted data symbols on the training symbols. Although such an investigation has not been carried out in this paper, the

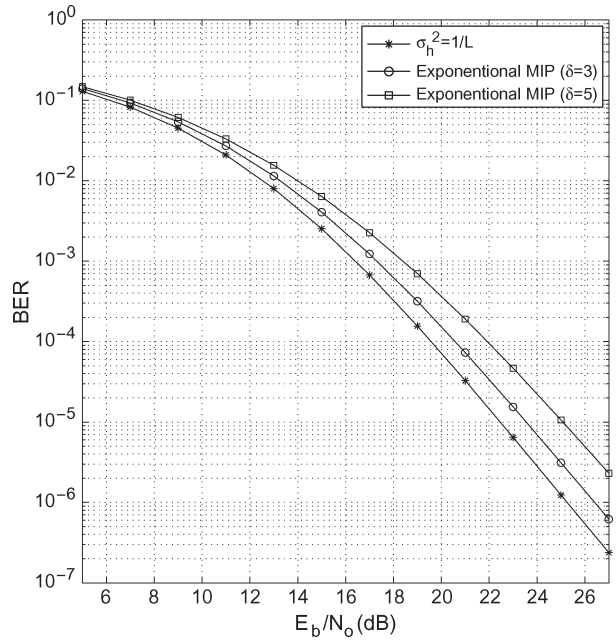

Fig. 8. BER performance of the proposed system considering different channel delay profiles. The STS system employs two transmit antennas and one receive antenna with $L = 2$ paths and PNR $= 5$ dB.

following argument provides some evidence that our scheme would achieve a higher capacity over the CP scheme. In our work, we fix the problem of poor channel estimation provided by SIP through violating the correlation between the pilot and data symbols by using a channel decorrelator. This enhances the quality of the channel estimates, which can be noticed from the perfect match of the BER curves of the proposed estimation and detection scheme, and the perfect channel-estimation case (see Fig. 5). Consequently, the employment of the enhanced SIP scheme (coupled with the channel decorrelator) guarantees the high accuracy of channel-estimation process, whether considering a low or high channel coherence time, which would achieve capacity gain over the CP scheme in both slow-and fast-fading channels. However, it should also be noted that there is a power penalty to obtain accurate channel estimates.

VII. Conclusion

We have proposed a channel-estimation and data-detection technique for CDMA STS systems. Our scheme employs channel and data decorrelation prior to channel estimation and, hence, removes the effect of interference from the channel estimates. In particular, we have shown that the proposed scheme is robust to channel interference caused by the multiple-access transmission in asynchronous CDMA uplinks. The performance of the proposed receiver structure has been studied over a frequency-selective fading channel for a two-transmit-antenna and V-receive-antenna configuration. We have derived the probability of error for different antenna configurations. Through both simulations and analytical results, we have proven that our estimation technique is able to deliver the full system diversity.

APPENDIX A
DEFINITION OF PILOT AND DATA CODE MATRICES

We construct the pilot and data matrices with the aid of Fig. 2. In (2), the nonzero elements in $\mathbf{C}[0]$ include the periods of the transmitted sequences with a blank background in Fig. 2. Therefore, $\mathbf{C}_k[0]$ is defined by (49), shown at the bottom of the page, where $\mathbf{0}$ represents a zero matrix, and $\Delta\tau_k = \tau_{\max} - \tau_k$. From Fig. 2, the nonzero elements in $\mathbf{C}[1]$ include the periods of the transmitted sequences with downward diagonal background. Hence, $\mathbf{C}_k[1]$ $(k = 1, 2, \ldots, K)$ is given by (50), shown at the bottom of the page. Similarly, during the data detection, $\mathbf{C}'[0]$ is given by

$$\mathbf{C}'[0] = [\mathbf{C}'_1[0], \mathbf{C}'_2[0], \ldots, \mathbf{C}'_K[0]]$$

with $\mathbf{C}'_k[0]$ being defined by (51), shown at the bottom of the page, and

$$\mathbf{C}'[1] = [\mathbf{C}'_1[1], \mathbf{C}'_2[1], \ldots, \mathbf{C}'_K[1]]$$

$$\mathbf{C}_k[0] = \begin{bmatrix}
 & \mathbf{0}_{\tau_k\times 4} & & & & \mathbf{0}_{\tau_k\times 4} & \cdots & & \mathbf{0}_{\tau_k\times 4} & & \\
P_{k1}^0 & P_{k2}^0 & c_{k1}^0 & c_{k2}^0 & 0 & 0 & \cdots & 0 & 0 & 0 & 0 \\
P_{k1}^1 & P_{k2}^1 & c_{k1}^1 & c_{k2}^1 & P_{k1}^0 & P_{k2}^0 & \cdots & 0 & 0 & 0 & 0 \\
\vdots & \cdots & \cdots & \vdots & \vdots & \cdots & \ddots & \vdots & \cdots & \cdots & \vdots \\
\vdots & \cdots & \cdots & \vdots & \vdots & \cdots & \ddots & P_{k1}^0 & P_{k2}^0 & c_{k1}^0 & c_{k2}^0 \\
\vdots & \cdots & \cdots & \vdots & \vdots & \cdots & \ddots & \vdots & \cdots & \cdots & \vdots \\
P_{k1}^{2N-1} & P_{k2}^{2N-1} & c_{k1}^{2N-1} & c_{k2}^{2N-1} & P_{k1}^{2N-2} & P_{k2}^{2N-2} & \cdots & P_{k1}^{2N-L} & P_{k2}^{2N-L} & c_{k1}^{2N-L} & c_{k2}^{2N-L} \\
0 & 0 & 0 & 0 & P_{k1}^{2N-1} & P_{k2}^{2N-1} & \cdots & P_{k1}^{2N-L+1} & P_{k2}^{2N-L+1} & c_{k1}^{2N-L+1} & c_{k2}^{2N-L+1} \\
0 & 0 & 0 & 0 & 0 & 0 & \cdots & P_{k1}^{2N-L+2} & P_{k2}^{2N-L+2} & c_{k1}^{2N-L+2} & c_{k2}^{2N-L+2} \\
\vdots & \cdots & \cdots & \vdots & \vdots & \cdots & \ddots & \vdots & \cdots & \cdots & \vdots \\
0 & \cdots & \cdots & 0 & 0 & \cdots & \cdots & P_{k1}^{2N-1} & P_{k2}^{2N-1} & c_{k1}^{2N-1} & c_{k2}^{2N-1} \\
 & \mathbf{0}_{\Delta\tau_k\times 4} & & & & \mathbf{0}_{\Delta\tau_k\times 4} & \cdots & & \mathbf{0}_{\Delta\tau_k\times 4} & &
\end{bmatrix} \tag{49}$$

$$\mathbf{C}_k[1] = \begin{bmatrix}
\mathbf{0}_{(2N+\tau_k)\times 4} & & & & \mathbf{0}_{(2N+\tau_k)\times 4} & & .. & \mathbf{0}_{(2N+\tau_k)\times 4} & & & \\
P_{k1}^0 & P_{k2}^0 & c_{k1}^0 & c_{k2}^0 & 0 & 0 & .. & 0 & 0 & 0 & 0 \\
P_{k1}^1 & P_{k2}^1 & c_{k1}^1 & c_{k2}^1 & P_{k1}^0 & P_{k2}^0 & .. & 0 & 0 & 0 & 0 \\
\vdots & \cdots & \cdots & \vdots & \vdots & \cdots & \ddots & \vdots & .. & .. & \vdots \\
P_{k1}^{L-1} & P_{k2}^{L-1} & c_{k1}^{L-1} & c_{k2}^{L-1} & P_{k1}^{L-2} & \cdots & \ddots & P_{k1}^0 & .. & .. & c_{k2}^0 \\
\vdots & \cdots & \cdots & \vdots & \vdots & \cdots & \ddots & \vdots & .. & .. & \vdots \\
P_{k1}^{\Delta\tau_k+L-2} & P_{k2}^{\Delta\tau_k+L-2} & c_{k1}^{\Delta\tau_k+L-2} & c_{k2}^{\Delta\tau_k+L-2} & P_{k1}^{\Delta\tau_k+L-3} & \cdots & .. & P_{k1}^{\Delta\tau_k-1} & .. & .. & c_{k2}^{\Delta\tau_k-1}
\end{bmatrix} \tag{50}$$

$$\mathbf{C}'_k[0] = \begin{bmatrix}
\mathbf{0}_{\tau_k\times 2} & & \mathbf{0}_{\tau_k\times 2} & & \cdots & \mathbf{0}_{\tau_k\times 2} & \\
c_{k1}^0 & c_{k2}^0 & 0 & 0 & \cdots & 0 & 0 \\
c_{k1}^1 & c_{k2}^1 & c_{k1}^0 & c_{k2}^0 & \cdots & 0 & 0 \\
c_{k1}^2 & c_{k2}^2 & c_{k1}^1 & c_{k2}^1 & \cdots & 0 & 0 \\
\vdots & \vdots & \vdots & \vdots & \ddots & \vdots & \vdots \\
\vdots & \vdots & \vdots & \vdots & \ddots & c_{k1}^0 & c_{k2}^0 \\
\vdots & \vdots & \vdots & \vdots & \ddots & \vdots & \vdots \\
c_{k1}^{2N-1} & c_{k2}^{2N-1} & c_{k1}^{2N-2} & c_{k2}^{2N-2} & \cdots & c_{k1}^{2N-L} & c_{k2}^{2N-L} \\
0 & 0 & c_{k1}^{2N-1} & c_{k2}^{2N-1} & \cdots & c_{k1}^{2N-L+1} & c_{k2}^{2N-L+1} \\
0 & 0 & 0 & 0 & \cdots & c_{k1}^{2N-L+2} & c_{k2}^{2N-L+2} \\
\vdots & \vdots & \vdots & \vdots & \ddots & \vdots & \vdots \\
0 & 0 & 0 & 0 & \cdots & c_{k1}^{2N-1} & c_{k2}^{2N-1} \\
\mathbf{0}_{\Delta\tau_k\times 2} & & \mathbf{0}_{\Delta\tau_k\times 2} & & \cdots & \mathbf{0}_{\Delta\tau_k\times 2} &
\end{bmatrix} \tag{51}$$

where $\mathbf{C}'_k[1]$ is defined by (52), shown at the bottom of the page. In (8)–(10), $\mathbf{C}'[-1]$ is the $[(2N+L-1+\tau_{\max})\times 2LK]$ data code matrix, which includes the data sequences corresponding to the K users of the previous STS symbols within the current observation interval. From Fig. 2, the nonzero elements in $\mathbf{C}'[-1]$ include the periods of the transmitted sequences with small grid background, i.e.,

$$\mathbf{C}'[-1] = [\mathbf{C}'_1[-1], \mathbf{C}'_2[-1], \ldots, \mathbf{C}'_K[-1]]$$

where $\mathbf{C}'_k[-1]$ is given by (53), shown at the bottom of the page.

Appendix B
Covariance Matrix of $\mathbf{X}^v$

The covariance matrix of $\mathbf{X}^v$ in (31), at the vth receive antenna, is defined as

$$\mathbf{R} = E\left[\mathbf{X}^v \mathbf{X}^{vH}\right] = \begin{bmatrix} \mathbf{R}_{H-H} & \mathbf{0}_{2L\times 2LK} & \mathbf{0}_{2L\times 2L} \\ \mathbf{0}_{2LK\times 2L} & \mathbf{R}_{E-E} & \mathbf{0}_{2LK\times 2L} \\ \mathbf{0}_{2L\times 2L} & \mathbf{0}_{2L\times 2LK} & \mathbf{R}_{N-N} \end{bmatrix}$$

where $\mathbf{R}_{H-H}$, $\mathbf{R}_{E-E}$, and $\mathbf{R}_{N-N}$ represent the cross-correlation matrices corresponding to the channel coefficients of the first user, the channel estimation errors corresponding to the K-user system, and the noise samples at the data decorrelator output of the first user, respectively.

Let

$$\mathbf{h}^v = \left[h_{11}^{1,v}, h_{21}^{1,v}, h_{12}^{1,v}, \ldots, h_{2L}^{1,v}\right]^T$$
$$\mathbf{E}^{v'} = \left[e_{11}^{1,v}, e_{21}^{1,v}, \ldots, e_{2L}^{1,v}, \ldots, e_{2L}^{K,v}\right]^T$$
$$\mathbf{N}^v = \left[(\mathbf{N}_{dd}^v)_{1,1}, (\mathbf{N}_{dd}^v)_{2,1}, \ldots, (\mathbf{N}_{dd}^v)_{2L-1,1}, (\mathbf{N}_{dd}^v)_{2L,1}\right]^T.$$

Then

$$\mathbf{R}_{H-H} = E\left[\mathbf{h}^v \mathbf{h}^{vH}\right] = \begin{bmatrix} \sigma_h^2 & 0 & \cdots & 0 \\ 0 & \sigma_h^2 & \cdots & 0 \\ \vdots & \cdots & \cdots & \vdots \\ 0 & 0 & \cdots & \sigma_h^2 \end{bmatrix}$$

and $\mathbf{R}_{E-E}$ and $\mathbf{R}_{N-N}$ are defined in (54) and (55), shown at the top of the next page.

Appendix C
Coefficient Matrices $\mathbf{S}_1$ and $\mathbf{S}_2$

$\mathbf{S}_1$ is a square matrix of dimension $[4L+2LK]$, consisting of the coefficients corresponding to the elements of $\mathbf{X}^v$ in (29), and is given by

$$\mathbf{S}_1 = \begin{bmatrix} \mathbf{S}_{H-H} & \mathbf{S}_{H-E} & \mathbf{S}_{H-N} \\ \mathbf{S}_{H-E}^T & \mathbf{S}_{E-E} & \mathbf{S}_{E-N} \\ \mathbf{S}_{H-N}^T & \mathbf{S}_{E-N}^T & \mathbf{0}_{2L\times 2L} \end{bmatrix}$$

where

$$\mathbf{S}_{H-H(2L\times 2L)} = \begin{bmatrix} A & 0 & \cdots & 0 \\ 0 & A & \cdots & 0 \\ \vdots & \cdots & \cdots & \vdots \\ 0 & 0 & \cdots & A \end{bmatrix}$$

$$\mathbf{S}_{H-N(2L\times 2L)} = \begin{bmatrix} \frac{1}{2} & 0 & \cdots & 0 \\ 0 & -\frac{1}{2} & \cdots & 0 \\ \vdots & \cdots & \cdots & \vdots \\ 0 & 0 & \cdots & -\frac{1}{2} \end{bmatrix}$$

$$\mathbf{C}'_k[1] = \begin{bmatrix} \mathbf{0}_{(2N+\tau_k)\times 2} & & \mathbf{0}_{(2N+\tau_k)\times 2} & & \cdots & \mathbf{0}_{(2N+\tau_k)\times 2} & \\ c_{k1}^0 & c_{k2}^0 & 0 & 0 & \cdots & 0 & 0 \\ c_{k1}^1 & c_{k2}^1 & c_{k1}^0 & c_{k2}^0 & \cdots & 0 & 0 \\ c_{k1}^2 & c_{k2}^2 & c_{k1}^1 & c_{k2}^1 & \cdots & 0 & 0 \\ \vdots & \vdots & \vdots & \vdots & \ddots & \vdots & \vdots \\ c_{k1}^{L-1} & c_{k2}^{L-1} & c_{k1}^{L-2} & c_{k2}^{L-2} & \ddots & c_{k1}^0 & c_{k2}^0 \\ \vdots & \vdots & \vdots & \vdots & \ddots & \vdots & \vdots \\ c_{k1}^{\Delta\tau_k+L-2} & c_{k2}^{\Delta\tau_k+L-2} & c_{k1}^{\Delta\tau_k+L-3} & c_{k2}^{\Delta\tau_k+L-3} & \cdots & c_{k1}^{\Delta\tau_k-1} & c_{k2}^{\Delta\tau_k-1} \end{bmatrix} \tag{52}$$

$$\mathbf{C}'_k[-1] = \begin{bmatrix} c_{k1}^{2N-\tau_k} & c_{k2}^{2N-\tau_k} & c_{k1}^{2N-\tau_k-1} & c_{k2}^{2N-\tau_k-1} & \cdots & c_{k1}^{2N-\tau_k-L+1} & c_{k2}^{2N-\tau_k-L+1} \\ c_{k1}^{2N-\tau_k+1} & c_{k2}^{2N-\tau_k+1} & c_{k1}^{2N-\tau_k} & c_{k2}^{2N-\tau_k} & \cdots & c_{k1}^{2N-\tau_k-L+2} & c_{k2}^{2N-\tau_k-L+2} \\ \vdots & \vdots & \vdots & \vdots & \ddots & \vdots & \vdots \\ c_{k1}^{2N-1} & c_{k2}^{2N-1} & c_{k1}^{2N-2} & c_{k2}^{2N-2} & \cdots & c_{k1}^{2N-L} & c_{k2}^{2N-L} \\ 0 & 0 & c_{k1}^{2N-1} & c_{k2}^{2N-1} & \cdots & c_{k1}^{2N-L+1} & c_{k2}^{2N-L+1} \\ 0 & 0 & 0 & 0 & \cdots & c_{k1}^{2N-L+2} & c_{k2}^{2N-L+2} \\ \vdots & \vdots & \vdots & \vdots & \ddots & \vdots & \vdots \\ 0 & 0 & 0 & 0 & \cdots & c_{k1}^{2N-1} & c_{k2}^{2N-1} \\ \mathbf{0}_{(2N+\Delta_k)\times 2} & & \mathbf{0}_{(2N+\Delta_k)\times 2} & & \cdots & \mathbf{0}_{(2N+\Delta_k)\times 2} & \end{bmatrix} \tag{53}$$

$$\mathbf{R}_{E-E} = E\left[\mathbf{E}^{v'}\mathbf{E}^{v'H}\right] = \frac{1}{B^2}\begin{bmatrix} \left(\mathbf{R_p}^{-H}\right)_{1,1} & \left(\mathbf{R}_p^{-H}\right)_{1,2} & \left(\mathbf{R}_p^{-H}\right)_{1,5} & \cdots & \left(\mathbf{R}_p^{-H}\right)_{1,4LK-2} \\ \left(\mathbf{R}_p^{-H}\right)_{2,1} & \left(\mathbf{R}_p^{-H}\right)_{2,2} & \left(\mathbf{R}_p^{-H}\right)_{2,5} & \cdots & \left(\mathbf{R}_p^{-H}\right)_{2,4LK-2} \\ \vdots & \cdots & \cdots & \cdots & \vdots \\ \left(\mathbf{R}_p^{-H}\right)_{4L-2,1} & \left(\mathbf{R}_p^{-H}\right)_{4L-2,2} & \left(\mathbf{R}_p^{-H}\right)_{4L-2,5} & \cdots & \left(\mathbf{R}_p^{-H}\right)_{4L-2,4LK-2} \\ \vdots & \cdots & \cdots & \cdots & \vdots \\ \left(\mathbf{R}_p^{-H}\right)_{4LK-2,1} & \left(\mathbf{R}_p^{-H}\right)_{4LK-2,2} & \left(\mathbf{R}_p^{-H}\right)_{4LK-2,5} & \cdots & \left(\mathbf{R}_p^{-H}\right)_{4LK-2,4LK-2} \end{bmatrix} \tag{54}$$

$$\mathbf{R}_{N-N} = E\left[\mathbf{N}^{v}\mathbf{N}^{vH}\right] = \begin{bmatrix} \left(\mathbf{R}_d^{-H}\right)_{1,1} & \left(\mathbf{R}_d^{-H}\right)_{1,2} & \cdots & \left(\mathbf{R}_d^{-H}\right)_{1,2L} \\ \left(\mathbf{R}_d^{-H}\right)_{2,1} & \left(\mathbf{R}_d^{-H}\right)_{2,2} & \cdots & \left(\mathbf{R}_d^{-H}\right)_{2,2L} \\ \vdots & \cdots & \cdots & \vdots \\ \left(\mathbf{R}_d^{-H}\right)_{2L,1} & \left(\mathbf{R}_d^{-H}\right)_{2L,2} & \cdots & \left(\mathbf{R}_d^{-H}\right)_{2L,2L} \end{bmatrix} \tag{55}$$

$$\mathbf{S}^{(1)}_{H-E(2L\times 2LK)} = \begin{bmatrix} \frac{-B\mathbf{X}_1(1)+A}{2} & \frac{-B\mathbf{X}_1(2)-A}{2} & \frac{-B\mathbf{X}_1(3)}{2} & \cdots & \cdots & \cdots & \frac{-B\mathbf{X}_1(2LK)}{2} \\ \frac{B\mathbf{X}_2(1)+A}{2} & \frac{B\mathbf{X}_2(2)+A}{2} & \frac{B\mathbf{X}_2(3)}{2} & \cdots & \cdots & \cdots & \frac{B\mathbf{X}_2(2LK)}{2} \\ \frac{-B\mathbf{X}_3(1)}{2} & \frac{-B\mathbf{X}_3(2)}{2} & \frac{-B\mathbf{X}_3(3)+A}{2} & \cdots & \cdots & \cdots & \frac{-B\mathbf{X}_3(2LK)}{2} \\ \vdots & \cdots & \cdots & \cdots & \cdots & \cdots & \vdots \\ \frac{B\mathbf{X}_{2L}(1)}{2} & \frac{B\mathbf{X}_{2L}(2)}{2} & \cdots & \cdots & \frac{B\mathbf{X}_{2L}(2L)+A}{2} & \cdots & \frac{B\mathbf{X}_{2L}(2LK)}{2} \end{bmatrix} \tag{56}$$

$$\mathbf{S}_{E-E(2LK\times 2LK)} = \begin{bmatrix} -B\mathbf{X}_1(1) & \frac{-B\mathbf{X}_1(2)+B\mathbf{X}_2(1)}{2} & \cdots & \frac{-B\mathbf{X}_1(2L)+B\mathbf{X}_{2L}(1)}{2} & \cdots & \cdots & \frac{-B\mathbf{X}_1(2LK)}{2} \\ \frac{B\mathbf{X}_2(1)-B\mathbf{X}_1(2)}{2} & B\mathbf{X}_2(2) & \cdots & \frac{B\mathbf{X}_2(2L)+B\mathbf{X}_{2L}(2)}{2} & \cdots & \cdots & \frac{B\mathbf{X}_2(2LK)}{2} \\ \frac{-B\mathbf{X}_3(1)-B\mathbf{X}_1(3)}{2} & \frac{-B\mathbf{X}_3(2)+B\mathbf{X}_2(3)}{2} & \cdots & \frac{-B\mathbf{X}_3(2L)+B\mathbf{X}_{2L}(3)}{2} & \cdots & \cdots & \frac{-B\mathbf{X}_3(2LK)}{2} \\ \vdots & \cdots & \cdots & \cdots & \cdots & \cdots & \vdots \\ \frac{B\mathbf{X}_{2L}(1)-B\mathbf{X}_1(2L)}{2} & \frac{B\mathbf{X}_{2L}(2)+B\mathbf{X}_2(2L)}{2} & \cdots & B\mathbf{X}_{2L}(2L) & \cdots & \cdots & \frac{B\mathbf{X}_2(2LK)}{2} \\ \frac{-B\mathbf{X}_1(2L+1)}{2} & \frac{B\mathbf{X}_2(2L+1)}{2} & \cdots & \frac{B\mathbf{X}_{2L}(2L+1)}{2} & 0 & \cdots & 0 \\ \vdots & \cdots & \cdots & \cdots & \cdots & \cdots & \vdots \\ \frac{-B\mathbf{X}_1(2LK)}{2} & \frac{B\mathbf{X}_2(2LK)}{2} & \cdots & \frac{B\mathbf{X}_{2L}(2LK)}{2} & 0 & \cdots & 0 \end{bmatrix} \tag{57}$$

$$\mathbf{S}^{(2)}_{H-E(2L\times 2LK)} = \begin{bmatrix} \frac{-B\mathbf{X}_1(1)+A}{2} & \frac{-B\mathbf{X}_1(2)+A}{2} & \frac{-B\mathbf{X}_1(3)}{2} & \cdots & \cdots & \cdots & \frac{-B\mathbf{X}_1(2LK)}{2} \\ \frac{B\mathbf{X}_2(1)-A}{2} & \frac{B\mathbf{X}_2(2)+A}{2} & \frac{B\mathbf{X}_2(3)}{2} & \cdots & \cdots & \cdots & \frac{B\mathbf{X}_2(2LK)}{2} \\ \frac{-B\mathbf{X}_3(1)}{2} & \frac{-B\mathbf{X}_3(2)}{2} & \frac{-B\mathbf{X}_3(3)+A}{2} & \cdots & \cdots & \cdots & \frac{-B\mathbf{X}_3(2LK)}{2} \\ \vdots & \cdots & \cdots & \cdots & \cdots & \cdots & \vdots \\ \frac{B\mathbf{X}_{2L}(1)}{2} & \frac{B\mathbf{X}_{2L}(2)}{2} & \cdots & \cdots & \frac{B\mathbf{X}_{2L}(2L)+A}{2} & \cdots & \frac{B\mathbf{X}_{2L}(2LK)}{2} \end{bmatrix} \tag{58}$$

$$\mathbf{S}_{E-N(2LK\times 2L)} = \begin{bmatrix} \frac{1}{2} & 0 & \cdots & 0 \\ 0 & -\frac{1}{2} & \cdots & 0 \\ \vdots & \cdots & \cdots & \vdots \\ 0 & 0 & \cdots & -\frac{1}{2} \\ 0 & 0 & \cdots & 0 \\ \vdots & \cdots & \cdots & \vdots \\ 0 & 0 & \cdots & 0 \end{bmatrix}.$$

Finally, $\mathbf{S}_{H-E}$ and $\mathbf{S}_{E-E}$ are given by (56) and (57), shown at the top of the page, respectively. Similarly, one can find the coefficient matrix $\mathbf{S}_2$ with submatrices having the same definitions as the corresponding submatrices in $\mathbf{S}_1$, except $\mathbf{S}_{H-E}$, which is defined by (58), shown at the top of the page.

REFERENCES

[1] Z. Zvonar and D. Brady, "Coherent and differently coherent multiuser detectors for asynchronous CDMA frequency selective channels," in *Proc. IEEE MILCOM*, Oct. 1992, pp. 442–446.

[2] Z. Liu, G. B. Giannakis, B. Muquet, and S. Zhou, "Space-time coding for broadband wireless communications," *Wireless Syst. Mobile Comput.*, vol. 1, no. 1, pp. 33–53, Jan.–Mar. 2001.

[3] A. F. Naguib, V. Tarokh, N. Seshadri, and A. R. Calderbank, "A space-time coding modem for high-data-rate wireless communications," *IEEE J. Sel. Areas in Commun.*, vol. 16, no. 8, pp. 1459–1478, Aug. 1998.

[4] V. Tarokh, N. Seshadri, and A. R. Calderbank, "Space-time codes for high data rate wireless communication: Performance criterion and code construction," *IEEE Trans. Inf. Theory*, vol. 44, no. 2, pp. 744–765, Mar. 1998.
[5] S. M. Alamouti, "A simple transmit diversity technique for wireless communications," *IEEE J. Sel. Areas Commun.*, vol. 16, no. 8, pp. 1451–1458, Oct. 1998.
[6] V. Tarokh, H. Jafarkhani, and A. R. Calderbank, "Space-time block codes from orthogonal designs," *IEEE Trans. Inf. Theory*, vol. 45, no. 5, pp. 1456–1467, Jul. 1999.
[7] M. J. Juntti and M. Latva-aho, "Multiuser receivers for CDMA systems in Rayleigh fading channels," *IEEE Trans. Veh. Technol.*, vol. 49, no. 3, pp. 885–899, May 2000.
[8] B. Hochwald, T. Marzetta, and C. Papadias, "A transmitter diversity scheme for wideband CDMA systems based on space-time spreading," *IEEE J. Sel. Areas Commun.*, vol. 19, no. 1, pp. 1451–1458, Jan. 2001.
[9] L.-L. Yang, "MIMO-assisted space-code-division multiple-access: Linear detectors and performance over multipath fading channels," *IEEE J. Sel. Areas Commun.*, vol. 24, no. 1, pp. 121–131, Jan. 2006.
[10] G. V. V. Sharma and A. Chockalingam, "Performance analysis of maximum-likelihood multiuser detection in space-time-coded CDMA with imperfect channel estimation," *IEEE Trans. Veh. Technol.*, vol. 55, no. 6, pp. 1824–1837, Nov. 2006.
[11] H. Shuangchi, J. K. Tugnait, and M. Xiaohong, "On superimposed training for MIMO channel estimation and symbol detection," *IEEE Trans. Signal Process.*, vol. 55, no. 6, pp. 3007–3021, Jun. 2007.
[12] A. L. Swindlehurst and G. Leus, "Blind and semi-blind equalization for generalized space-time block codes," *IEEE Trans. Signal Process.*, vol. 50, no. 10, pp. 2489–2498, Oct. 2002.
[13] Y. Sung, L. Tong, and A. Swami, "Blind channel estimation for space-time coded WCDMA," *EURASIP J. Wireless Commun. Netw.*, vol. 2004, no. 2, pp. 322–334, Dec. 2004.
[14] X. Gao, B. Jiang, X. You, Z. Pan, and Y. Xue, "Efficient channel estimation for MIMO single-carrier block transmission with dual cyclic timeslot structure," *IEEE Trans. Commun.*, vol. 55, no. 11, pp. 2210–2223, Nov. 2007.
[15] X. Meng, J. K. Tugnait, and S. He, "Iterative joint channel estimation and data detection using superimposed training: Algorithms and performance analysis," *IEEE Trans. Veh. Technol.*, vol. 56, no. 4, pp. 1873–1880, Jul. 2007.
[16] L. Chong and L. Milstein, "The effects of channel-estimation errors on a space-time spreading CDMA system with dual transmit and dual receive diversity," *IEEE Trans. Commun.*, vol. 52, no. 7, pp. 1145–1151, Jul. 2004.
[17] R. Lupas and S. Verdu, "Near-far resistance of multiuser detectors in asynchronous channels," *IEEE Trans. Commun.*, vol. 38, no. 4, pp. 496–508, Apr. 1990.
[18] S. Haykin, *Array Signal Processing*. Englewood Cliffs, NJ: Prentice-Hall, 1984.
[19] Y.-P. Cheng, K.-Y. Zhang, and Z. Xu, *Matrix Theory*. Xi'an, China: Northwestern Polytech. Univ. Press, 2002.
[20] G. Golub and A. V. Loan, *Matrix Computations*. Baltimore, MD: Johns Hopkins Univ. Press, 1996.
[21] S. Verdu, *Multiuser Detection*. Cambridge, U.K.: Cambridge Univ. Press, 1998.
[22] C. A. Balanis, *Antenna Theory: Analysis and Design*. Hoboken, NJ: Wiley, 2005.
[23] R. A. Soni and R. M. Buehrer, "On the performance of open-loop transmit diversity techniques for IS-2000 systems: Comparative study," *IEEE Trans. Wireless Commun.*, vol. 3, no. 5, pp. 1602–1615, Sep. 2004.
[24] G. L. Turin, "The characteristic function of Hermitian quadratic forms in complex normal variables," *Biometrika*, vol. 47, no. 1/2, pp. 199–201, Jun. 1960.
[25] A. Papoulis and S. U. Pillai, *Probability, Random Variables and Stochastic Processes*. New York: McGraw-Hill, 2002.
[26] M. J. Barrett, "Error probability for optimal and suboptimal quadratic receivers in rapid Rayleigh fading channels," *IEEE J. Sel. Areas Commun.*, vol. SAC-5, no. 2, pp. 302–304, Feb. 1987.
[27] D. G. Zill and M. R. Cullen, *Advanced Engineering Mathematics*. Sudbury, MA: Jones & Bartlett, 2006.
[28] O. Brugia, "A noniterative method for the partial fraction expansion of a rational function with high order poles," *SIAM Rev.*, vol. 7, no. 3, pp. 381–387, Jul. 1965.
[29] L. L. Chong and L. B. Milstein, "Convolutionally coded multicarrier DS-CDMA with imperfect channel estimation," in *Proc. 39th Allerton Conf. Commun., Control, Comput.*, Oct. 2001, pp. 543–552.
[30] A. Russ and M. K. Varanasi, "Noncoherent multiuser detection for nonlinear modulation over the Rayleigh fading channel," *IEEE Trans. Inf. Theory*, vol. 47, no. 1, pp. 295–307, Jan. 2001.
[31] M. Brehler and M. K. Varanasi, "Asymptotic error probability analysis of quadratic receivers in Rayleigh-fading channels with applications to a unified analysis of coherent and noncoherent space-time receivers," *IEEE Trans. Inf. Theory*, vol. 47, no. 6, pp. 2383–2399, Sep. 2001.
[32] M. Coldrey and P. Bohlin, "Training-based MIMO systems—Part I: Performance comparison," *IEEE Trans. Signal Process.*, vol. 55, no. 11, pp. 5464–5476, Nov. 2007.

Ayman Assra received the B.Sc. degree in electrical engineering from Alexandria University, Alexandria, Egypt, in 2000 and the M.Sc. degree from the Arab Academy for Science and Technology and Maritime Transport, Alexandria, in 2004. He is currently working toward the Ph.D. degree in electrical and computer engineering wth Concordia University, Montreal, QC, Canada.

Since May 2005, he has been a Research Assistant with the Department of Electrical and Computer Engineering, Concordia University. His current research interests include space-time processing and multiple-input–multiple-output communications.

Walaa Hamouda (SM'06) received the M.A.Sc. and Ph.D. degrees in electrical and computer engineering from Queen's University, Kingston, ON, Canada, in 1998 and 2002, respectively.

In July 2002, he joined the Department of Electrical and Computer Engineering, Concordia University, Montreal, QC, Canada, where he is currently an Associate Professor. Since June 2006, he has been the Concordia University Research Chair in Communications and Networking. He is an Associate editor of the *Wiley International Journal of Communication Systems* and the *Journal of Computer Systems, Networks, and Communications*. His current research interests include wireless networks, multiple-input–multiple-output space-time processing, multiuser communications, cross-layer design, and source and channel coding.

Dr. Hamouda has received many awards, including the best paper award (WNS) of the 2009 International Conference on Communications (ICC) and the IEEE Canada Certificate of Appreciation in 2007 and 2008. He served as the Technical Cochair of the Ad hoc, Sensor, and Mesh Networking Symposium of the 2010 IEEE ICC and the 25th Queen's Biennial Symposium on Communications, as well as the Track Chair for the Radio Access Techniques of the Fall 2006 IEEE Vehicular Technology Conference. From September 2005 to November 2008, was the Chair of the IEEE Montreal Chapter of Communications and Information Theory. He serves as Associate Editor for the IEEE TRANSACTIONS ON VEHICULAR TECHNOLOGY and the IEEE COMMUNICATIONS LETTERS.

Amr Youssef (SM'06) received the B.Sc. and M.Sc. degrees from Cairo University, Cairo, Egypt, in 1990 and 1993, respectively, and the Ph.D. degree from Queens University, Kingston, ON, Canada, in 1997.

He is currently an Associate Professor with the Concordia Institute for Information Systems Engineering (CIISE), Concordia University, Montreal, QC, Canada. Before joining CIISE, he was with Nortel Networks; the Center for Applied Cryptographic Research, University of Waterloo, Waterloo, ON, Canada; IBM; and Cairo University. His research interests include cryptology, network security, and wireless communications.